Hindawi
International Journal of Intelligent Systems
Volume 2023, Article ID 8818233, 16 pages
https://doi.org/10.1155/2023/8818233

WILEY | Hindawi

Research Article

Distributed Fixed-Time Event-Triggered Consensus Control for Uncertain Nonlinear Multiagent Systems with Actuator Failures

Jianhui Wang,[1] **Chen Wang**,[1] **Kairui Chen**,[1,2] **and Zitao Chen**[1]

[1]*School of Mechanical and Electrical Engineering, Guangzhou University, Guangzhou, China*
[2]*School of Computer & Information, Qiannan Normal University for Nationalities, Guizhou, Duyun, China*

Correspondence should be addressed to Kairui Chen; kray@gzhu.edu.cn

Received 3 June 2023; Revised 13 July 2023; Accepted 8 August 2023; Published 24 August 2023

Academic Editor: Surya Prakash

A fixed-time event-triggered consensus control method is proposed for uncertain nonlinear multiagent systems with actuator failures. Since actuator failures, external disturbances and control gains are time-varying and completely unknown, the effects of these system constraints on the system are completely unknown, which makes the implementation of fixed-time tracking control challenging. To deal with these system constraints, radial basis function neural networks (RBFNNs) are applied to approximate the uncertain dynamics, and a boundary estimation method is presented to achieve adaptive compensation for them. Furthermore, considering that the implementation of this boundary estimation method requires a large number of communication resources, an event triggering mechanism is designed to reduce the update frequency of the controller. It is theoretically confirmed that using the proposed control scheme, all the followers can track the leader with sufficient accuracy in a predetermined time, and all the closed-loop signals are bounded. Finally, the simulation experiments verify the theoretical results.

1. Introduction

With the swift advancement of communication and computing technologies, the cooperative control of multiagent systems (MASs) has emerged as a research hotspot in the intelligent control field [1–3]. As consensus control is an important and fundamental issue of cooperative control, the scientific community has paid close attention to the consensus control in recent years [4–7]. The early works on consensus control focused on asymptotic consensus, which theoretically takes an infinitely long time to achieve uniform boundedness. For example, the consensus control was investigated for multiple Euler–Lagrange systems with disturbances in [5]. The leader-following consensus problem for MASs was addressed by an adaptive neural approach in [7], and the asymptotic consensus of the system was achieved. Recently, to improve the interference immunity and convergence speed of the system, scholars have proposed many finite-time consensus control methods [8–12]. Wang et al. [9] studied the finite-time consensus control scheme for second-order MASs with mismatched disturbances. Considering MASs under undirected graphs, Du et al. [10] proposed a distributed finite-time consensus control algorithm. Nevertheless, since the initial system states have an impact on the convergence time, these finite-time consensus control methods cannot obtain a fixed convergence time. To remedy this deficiency, the fixed-time control whose convergence time is independent of the initial system states was proposed in [13]. Because of this feature, it was applied to the cooperative control of MASs [14–18]. In [14], a summary of recent developments regarding fixed-time cooperative control was provided. Liu et al. [15] studied the fixed-time consensus tracking control for MASs with input delays. For second-order MASs with external disturbances, Liu et al. [17] investigated a fixed-time consensus control method.

An important aspect of achieving cooperative control is that the actuators work properly. Nevertheless, it is inevitable that actuator failures will occur over long periods of system operation. Fault-tolerant control is one of the most promising control techniques used to maintain system safety and performance in the event of an unexpected failure. In

recent years, scholars have proposed many fault-tolerant control methods to cope with actuator failures [19–23]. Considering rigid spacecraft systems with actuator failures, a fault-tolerant control method was presented in [20]. Considering nonlinear systems with actuator failures, the trajectory tracking problem was investigated in [21]. For fault-tolerant control methods for MASs, please refer to the literature [22, 23]. In contrast to the works mentioned above, which studied the time-invariant failure problem, the authors in [24, 25] investigated the compensation problem of time-varying failure for uncertain nonlinear systems and MASs, respectively. However, to the best of our knowledge, little work has been reported that explicitly addresses the issue of actuator failures and fixed-time convergence for nonlinear MAS. Therefore, it is significant to study fault-tolerant control methods for nonlinear MAS in the framework of fixed-time control.

On the other hand, the actual system requires high-frequency communication to accomplish control tasks, so a large number of communication resources are required. Because the communication resources of the system are limited, it is of great engineering value to study how to reduce the communication burden. Event-triggered control is of great interest to scholars because it can economize the communication resources. Up to now, many event-triggered control methods have been proposed [26–31]. Based on the event-triggered control framework, Zhang et al. [26] investigated the adaptive consensus control for MASs with actuator failures. In [27], to further save communication resources, the control signal's transmission bits are taken into account, and a 2-bit-triggered control technique for nonlinear MASs was developed. For more event-triggered control methods of nonlinear systems, please refer to the literature [29–31].

According to the previous analysis, there is little work on fixed-time event-triggered fault-tolerant control for uncertain nonlinear MASs, although there are many significant results on consensus control. In particular, this control problem becomes more interesting and challenging when there are unknown and time-varying control gains and external disturbances in the system. This study makes an effort to address this issue by taking inspiration from previous studies. The primary innovation of this study, as compared to previous research outcomes, is evident in the following two areas:

(1) The long-term operation of the control system may lead to actuator failures, which will affect system performance or even lead to instability. In this research, to cope with the effects of actuator failures, external disturbances, and time-varying control gains, a boundary estimation method is proposed to compensate for their effects on the system. In addition, considering the large amount of communication resources required to implement this compensation method, an event-triggered mechanism is designed to relieve the communication pressure.

(2) Considering the requirement for fast convergence in engineering applications, a fixed-time consensus control method is developed. The fixed-time stability of the system can be achieved by using the proposed method. In other words, even if the system is affected by actuator failures, time-varying control gains, and external disturbances, the tracking error of the system can converge to near the origin in a fixed time independent of the initial states.

The rest parts will be organized as follows: the system model and preliminaries are given in Section 2. Section 3 introduces the fixed-time event-triggered controller design and stability analysis. Simulations are shown in Section 4. Finally, the conclusion is presented in Section 5.

2. Models and Preliminaries

2.1. Model Formulation. In this research, MASs made up of one leader and N followers are considered. To facilitate the description, the leader is marked as 0, and followers are marked as $k (k = 1, 2, \ldots, N)$. The model of follower k is given as follows:

$$\begin{cases} \dot{x}_{k,1} = x_{k,2}, \\ g_k(t)\dot{x}_{k,2} = u_k + f_k\left(x_{k,1}, x_{k,2}\right) + d_k(t), \\ y_k = x_{k,1}, \end{cases} \tag{1}$$

where $x_{k,1} = [x_{k,11}, x_{k,21}, \ldots, x_{k,s1}]^T \in \mathbb{R}^s$ and $x_{k,2} = [x_{k,12}, x_{k,22}, \ldots, x_{k,s2}]^T \in \mathbb{R}^s$ are state vectors, s is a positive integer; $g_k(t) = \mathrm{diag}\{g_{k,1}(t), g_{k,2}(t), \ldots, g_{k,s}(t)\} \in \mathbb{R}^{s\times s}$ is an unknown and time-varying parameter vector; $f_k = [f_{k,1}, f_{k,2}, \ldots, f_{k,s}]^T \in \mathbb{R}^s$ represents an unknown and smooth nonlinear function vector; $d_k(t) = [d_{k,1}(t), d_{k,2}(t), \ldots, d_{k,s}(t)]^T \in \mathbb{R}^s$ is an unknown and continuous external disturbance; $u_k = [u_{k,1}, u_{k,2}, \ldots, u_{k,s}]^T \in \mathbb{R}^s$ and $y_k = [y_{k,1}, y_{k,2}, \ldots, y_{k,s}]^T \in \mathbb{R}^s$ represent the control input and system output, respectively.

In practice, a long period of operation inevitably leads to actuator failures. It can cause a difference in the actuator input $\overline{u}_{k,i}$ and the actuator output $u_{k,i}$, which can affect system performance. Inspired by the literature [32], this difference is modeled as follows:

$$u_{k,i} = \rho_{k,i}(t)\overline{u}_{k,i} + r_{k,i}(t), t \geq t_{k,if}, \tag{2}$$

where $i = 1, 2, \ldots, s$, $\rho_{k,i}(t)$ is the health factor; $r_{k,i}(t)$ is the uncontrollable parameter; $t_{k,if}$ denotes the moment when the actuator starts to fail, and it is an arbitrary moment.

Thus, considering failure mode (2), dynamic model (1) becomes

$$\begin{cases} \dot{x}_{k,1} = x_{k,2}, \\ g_k(t)\dot{x}_{k,2} = \rho_k(t)\overline{u}_k + r_k(t) + f_k\left(x_{k,1}, x_{k,2}\right) + d_k(t), \\ y_k = x_{k,1}, \end{cases} \tag{3}$$

where $\overline{u}_k = [\overline{u}_{k,1}, \overline{u}_{k,2}, \ldots, \overline{u}_{k,s}]^T \in \mathbb{R}^s$, $\rho_k(t) = \mathrm{diag}\{\rho_{k,1}(t), \rho_{k,2}(t), \ldots, \rho_{k,s}(t)\} \in \mathbb{R}^{s\times s}$, and $r_k(t) = [r_{k,1}(t), r_{k,2}(t), \ldots, r_{k,s}(t)]^T \in \mathbb{R}^s$.

Remark 1. Different from control schemes [19–21] in which the parameters of actuator failures are constants, the control scheme for uncertain MASs with time-varying actuator failures is studied in this research. In engineering applications, the degree of actuator failures tends to vary with time, so studying time-varying actuator failures is of more engineering value. It is worth mentioning that the actuator works properly (i.e., $u_{k,i} = \overline{u}_{k,i}$) when $t < t_{k,if}$. In addition, the normal working model $u_{k,i} = \overline{u}_{k,i}$ is consistent with the failure mode (2). During the design of the controller, the compensation mechanism for unknown actuator failures will be designed based on model (2).

Agents (leaders and followers) are connected by a known and directed communication topology. The directed communication topology can be described by $\mathcal{G}(\mathcal{A}, \mathcal{H}, \mathcal{E}, \mathcal{V})$, where $\mathcal{A} = [a_{kj}] \in \mathbb{R}^{N\times N}$ $(k, j \in \{1, 2, \ldots, N\})$ is the weighted adjacency matrix among followers; $\mathcal{H} = \mathrm{diag}\{h_1, h_2, \ldots, h_N\} \in \mathbb{R}^N$ is the weighted adjacency vector between followers with leader 0; $\mathcal{E} = \{0, 1, 2, \ldots, N\}$ represents the set of leaders and followers; $\mathcal{V} \subseteq \mathcal{E} \times \mathcal{E}$ is the set of edges. If $(j,k) \in \mathcal{V}$ and $j \neq k$ (follower k can receive the information from follower j), then $a_{kj} > 0$, otherwise, $a_{kj} = 0$. Thus, the neighbors of follower k is $\mathcal{N}_k = \{j \mid (j,k) \in \mathcal{V}\}$. If follower k can receive the information from leader 0, then $h_i > 0$, otherwise, $h_i = 0$. Then, one can obtain a matrix $\mathcal{D} = \mathrm{diag}\{d_1, d_2, \ldots, d_N\} \in \mathbb{R}^{N\times N}$ and a Laplacian matrix $\mathcal{L} = \mathcal{D} - \mathcal{A}$ where $d_i = \sum_{j=1}^N a_{ij}$, $i = 1, 2, \ldots, N$.

Therefore, we can define the coordinate transformation of follower k as follows:

$$e_{k,i1} = h_k\left(y_{k,i} - y_{0,i}\right) + \sum_{j=1}^{N} a_{kj}\left(y_{k,i} - y_{j,i}\right), \tag{4}$$

$$e_{k,i2} = x_{k,i2} - \alpha_{k,i1}, \tag{5}$$

where $i = 1, 2, \ldots, s$, $y_{0,i}$ is the leader's output; $e_{k,i1}$ is a synchronization error; $e_{k,i2}$ is a virtual error; $\alpha_{k,i1}$ is a virtual controller which will be designed.

Assumption 2 ([8]). All followers have a path from the leader to themselves. The leader's output $y_{0,i}(i = 1, 2, \ldots, s)$ is bounded and continuous, and its 2nd order derivative $\ddot{y}_{0,i}$ is available.

Assumption 3 ([32]). The time-varying parameter $g_{k,i}(t)(i = 1, 2, \ldots, s)$ is positive and bounded, and the external disturbance $d_{k,i}(t)(i = 1, 2, \ldots, s)$ is bounded, i.e., $0 \le \underline{g}_{k,i} < g_{k,i}(t) \le \overline{g}_{k,i}$, and $|d_{k,i}(t)| \le \overline{d}_{k,i}$, where $\underline{g}_{k,i}$, $\overline{g}_{k,i}$, and $\overline{d}_{k,i}$ are unknown positive constants.

Assumption 4 ([32]). The parameters of the failure model (2) $\rho_{k,i}(t)$ and $r_{k,i}(t)$ are continuous and unknown (when $t > t_{k,if}$), and they satisfy $0 < \rho_{k,i}(t) < 1$ and $|r_{k,i}(t)| \le \overline{r}_{k,i}$ with $\overline{r}_{k,i} > 0$.

Remark 5. Assumption 2 is common and reasonable in tracking control studies for uncertain nonlinear systems or MASs, and similar assumptions can be found in [29–31, 33]. As illustrated in Assumption 3, in this study, external disturbances and time-varying control gains are considered, which is more reasonable and practical, although it makes control tasks more difficult. In Assumption 4, the time at which the actuator begins to fail $t_{k,if}$ is unknown and this uncertainty together with the unknown and time-varying parameters $\rho_{k,i}(t)$ and $r_{k,i}(t)$ makes the controller design interesting and challenging.

2.2. Preliminaries

Lemma 6 ([34, 35]). *For $\epsilon \in \mathbb{R}$ and $\delta > 0$, one has $-\epsilon \tanh(\epsilon/\delta) \le 0$ and $0 \le |\epsilon| - \epsilon \tanh(\epsilon/\delta) \le 0.2785\delta$.*

Lemma 7 ([36]). *For $\epsilon_1 \in \mathbb{R}$, $\epsilon_2 \in \mathbb{R}$, $\rho_1 > 0$, $\rho_2 > 0$, and $k > 0$, one has $|\epsilon_1|^{\rho_1}|\epsilon_2|^{\rho_2} \le \rho_1/\rho_2 + \rho_1 k|\epsilon_1|^{\rho_1+\rho_2} + \rho_2/\rho_2 + \rho_1 k^{-\rho_1/\rho_2}|\epsilon_2|^{\rho_1+\rho_2}$.*

Lemma 8 ([36, 37]). *For $\kappa_i > 0$, $0 < a \le 1$, $1 < b < +\infty$, and $i = 1, 2, \ldots, n$, one has $(\sum_{i=1}^n \kappa_i)^a \le \sum_{i=1}^n \kappa_i^a$, $(\sum_{i=1}^n \kappa_i)^b \le 1/n^{1-b} \sum_{i=1}^n \kappa_i^b$.*

3. Main Results

3.1. Fixed-Time Controller. According to the previous analysis, follower k can only obtain local system state information, so the design of the distributed controller $\overline{u}_{k,i}$ is presented in this subsection describes.

Step 9. The first Lyapunov function is constructed as follows:

$$V_{k,i1} = \frac{1}{2}e_{k,i1}^2. \tag{6}$$

According to (4), the time derivative of $e_{k,i1}$ is

$$\dot{e}_{k,i1} = (h_k + d_k)x_{k,i2} - \sum_{j\in\mathcal{N}_k} a_{kj}x_{j,i2} - h_k\dot{y}_{0,i}. \tag{7}$$

Thus, one can obtain that

$$\dot{V}_{k,i1} = (h_k + d_k)e_{k,i1}e_{k,i2} + (h_k + d_k)e_{k,i1}\alpha_{k,i1} - \left(\sum_{j\in\mathcal{N}_k} a_{kj}x_{j,i2} + h_k\dot{y}_{0,i}\right)e_{k,i1}. \tag{8}$$

The virtual controller $\alpha_{k,i1}$ is designed as follows:

$$\alpha_{k,i1} = \frac{1}{h_k + d_k}\left(-b_{k,i1}e_{k,i1}^3 - c_{k,i1}e_{k,i1}^{2q-1} + \sum_{j\in\mathcal{N}_k} a_{kj}x_{j,i2} + h_k\dot{y}_{0,i}\right), \tag{9}$$

where $b_{k,i1}$ and $c_{k,i1}$ are positive design parameters.

Substituting (9) into (8) yields

$$\dot{V}_{k,i1} = -b_{k,i1}e_{k,i1}^4 - c_{k,i1}e_{k,i1}^{2q} + (h_k + d_k)e_{k,i1}e_{k,i2}. \tag{10}$$

Step 10. According to (3), $\dot{x}_{k,i2} = 1/g_{k,i}(\rho_{k,i}\overline{u}_{k,i} + r_{k,i} + f_{k,i} + d_{k,i})$. Then, we define functions $\eta_{k,i}(t) = 1/g_{k,i}(r_{k,i} + d_{k,i})$ and $\zeta_{k,i} = 1/g_{k,i}\rho_{k,i}$. According to Assumptions 2 and 3, $\eta_{k,i}$ and $\zeta_{k,i}$ are bounded. Thus, one can define the boundary $\overline{\eta}_{k,i} = \sup_{t\geq 0}\{|\eta_{k,i}|\} > 0$ and $\overline{\zeta}_{k,i} = 1/\underline{\zeta}_{k,i} > 0$ with $\underline{\zeta}_{k,i} = \inf_{t\geq 0}\{\zeta_{k,i}\} > 0$. Two adaptive parameters $\widehat{\eta}_{k,i}$ and $\widehat{\zeta}_{k,i}$ are defined to estimate $\overline{\eta}_{k,i}$ and $\overline{\zeta}_{k,i}$, and one can obtain estimation errors $\widetilde{\eta}_{k,i} = \overline{\eta}_{k,i} - \widehat{\eta}_{k,i}$ and $\widetilde{\zeta}_{k,i} = \overline{\zeta}_{k,i} - \widehat{\zeta}_{k,i}$.

Remark 11. In order to cope with actuator failures, unknown control gains, and external disturbances, two adaptive parameters $\widehat{\eta}_{k,i}$ and $\widehat{\zeta}_{k,i}$ are designed. This approach reduces the impact of these system constraints by estimating critical values. In the next step, two adaptive laws $\dot{\widehat{\eta}}_{k,i}$ and $\dot{\widehat{\zeta}}_{k,i}$ will be designed to achieve fixed-time stability.

The estimation of $\vartheta_{k,i} = \|W_{k,i}^*\|^2$ is defined as $\widehat{\vartheta}_{k,i}$, where $W_{k,i}^*$ is the ideal weight of RBFNNs. Then, $V_{k,i2}$ is defined as follows:

$$V_{k,i2} = V_{k,i1} + \frac{1}{2}e_{k,i2}^2 + \frac{1}{2\sigma_{k,i}}\widetilde{\eta}_{k,i}^2 + \frac{\zeta_{k,i}}{2\gamma_{k,i}}\widetilde{\zeta}_{k,i}^2 + \frac{1}{2l_{k,i}}\widetilde{\vartheta}_{k,i}^2, \tag{11}$$

where $\sigma_{k,i} > 0$, $\gamma_{k,i} > 0$, $l_{k,i} > 0$, and $\widetilde{\vartheta}_{k,i} = \vartheta_{k,i} - \widehat{\vartheta}_{k,i}$.

Calculating the derivative of $V_{k,i2}$ yields

$$\begin{aligned}\dot{V}_{k,i2} &= \dot{V}_{k,i1} + e_{k,i2}\left(\dot{x}_{k,i2} - \dot{\alpha}_{k,i1}\right) - \frac{1}{\sigma_{k,i}}\widetilde{\eta}_{k,i}\dot{\widehat{\eta}}_{k,i} - \frac{\zeta_{k,i}}{\gamma_{k,i}}\widetilde{\zeta}_{k,i}\dot{\widehat{\zeta}}_{k,i} - \frac{1}{l_{k,i}}\widetilde{\vartheta}_{k,i}\dot{\widehat{\vartheta}}_{k,i}\\ &\leq \dot{V}_{k,i1} + \zeta_{k,i}\overline{u}_{k,i}e_{k,i2} + \overline{\eta}_{k,i}|e_{k,i2}| + \overline{f}_{k,i}(\chi_{k,i})e_{k,i2} - \frac{1}{2}e_{k,i2}^2\\ &\quad - (h_k + d_k)e_{k,i1}e_{k,i2} - \frac{1}{\sigma_{k,i}}\widetilde{\eta}_{k,i}\dot{\widehat{\eta}}_{k,i} - \frac{\zeta_{k,i}}{\gamma_{k,i}}\widetilde{\zeta}_{k,i}\dot{\widehat{\zeta}}_{k,i} - \frac{1}{l_{k,i}}\widetilde{\vartheta}_{k,i}\dot{\widehat{\vartheta}}_{k,i},\end{aligned} \tag{12}$$

where $\overline{f}_{k,i}(\chi_{k,i}) = (h_k + d_k)e_{k,i1} + 1/g_{k,i}f_{k,i} + 1/2e_{k,i2} - \dot{\alpha}_{k,i1}$, $\chi_{k,i} = [x_{k,1}^T, x_{k,2}^T, x_{j,i1}, x_{j,i2}]^T$ $(j \in \mathcal{N}_k)$, and $\chi_{k,i} = [x_{k,1}^T, x_{k,2}^T, x_{j,i1}, x_{j,i2}, y_{0,i}, \dot{y}_{0,i}]^T$ if $(0,k) \in \mathcal{V}$. As $\overline{f}_{k,i}$ is a continuous function, it can be approximated by RBFNNs. Similar to [7], RBFNNs were used to estimate the uncertainty function as follows:

$$\overline{f}_{k,i}(\chi_{k,i}) = W_{k,i}^{*T}S_{k,i}(\chi_{k,i}) + \upsilon_{k,i}(\chi_{k,i}), \tag{13}$$

$W_{k,i}^* = [W_{k,i1}^*, W_{k,i2}^*, \ldots, W_{k,in}^*]^T$ and $S(\chi)_{k,i} = [S_{k,i1}(\chi), S_{k,i2}(\chi), \ldots, S_{k,n}(\chi)]^T$ are the ideal weight vector and the basis function vector, respectively. The approximation error $\upsilon_{k,i}(\chi_{k,i})$ satisfies $\upsilon_{k,i}(\chi_{k,i}) \leq \overline{\upsilon}_{k,i}$ with $\overline{\upsilon}_{k,i} > 0$.

Then, one can get

$$\overline{f}_{k,i}(\chi_{k,i})e_{k,i2} \leq \frac{1}{2\varepsilon_{k,i}^2}\vartheta_{k,i}\|S_{k,i}\|^2 e_{k,i2}^2 + \frac{1}{2}\varepsilon_{k,i}^2 + \frac{1}{2}e_{k,i2}^2 + \frac{1}{2}\overline{\upsilon}_{k,i}^2, \tag{14}$$

where $\varepsilon_{k,i} > 0$.

By substituting (14) into (12), one has

$$\begin{aligned}\dot{V}_{k,i2} \leq\ & -b_{k,i1}e_{k,i1}^4 - c_{k,i1}e_{k,i1}^{2q} + \zeta_{k,i}\overline{u}_{k,i}e_{k,i2} + \overline{\eta}_{k,i}|e_{k,i2}| + \frac{1}{2\varepsilon_{k,i}^2}\vartheta_{k,i}\|S_{k,i}\|^2 e_{k,i2}^2\\ &- \frac{1}{\sigma_{k,i}}\widetilde{\eta}_{k,i}\dot{\widehat{\eta}}_{k,i} - \frac{\zeta_{k,i}}{\gamma_{k,i}}\widetilde{\zeta}_{k,i}\dot{\widehat{\zeta}}_{k,i} - \frac{1}{l_{k,i}}\widetilde{\vartheta}_{k,i}\dot{\widehat{\vartheta}}_{k,i} + \frac{1}{2}\varepsilon_{k,i}^2 + \frac{1}{2}\overline{\upsilon}_{k,i}^2.\end{aligned} \tag{15}$$

In the traditional time-triggered mechanism, the actuator input $\overline{u}_{k,i}$ is updated periodically, which requires a lot of communication resources. In this study, a switching threshold event-triggered mechanism is designed to reduce the update frequency of $\overline{u}_{k,i}$. The event-triggered mechanism is defined as follows:

$$t_{k,i,z+1} = \begin{cases} \inf\left\{t \in \mathbb{R} \mid \left|m_{k,i}(t)\right| \geq s_{k,i1} + \varrho_{k,i}\left|\overline{u}_{k,i}(t)\right|\right\}, & \left|\overline{u}_{k,i}\right| \leq \Delta_{k,i}, \\ \inf\left\{t \in \mathbb{R} \mid \left|m_{k,i}(t)\right| \geq s_{k,i2}\right\}, & \left|\overline{u}_{k,i}\right| > \Delta_{k,i}, \end{cases} \tag{16}$$

$$\omega_{k,i}(t) = \begin{cases} -\alpha_{k,i2}\tanh\left(\frac{e_{k,i2}\alpha_{k,i2}}{\delta_{k,i}}\right)\left(1+\varrho_{k,i}\right) - \frac{\left(1+\varrho_{k,i}\right)e_{k,i2}}{2\left(1-\varrho_{k,i}\right)^2}, & \left|\overline{u}_{k,i}\right| \leq \Delta_{k,i}, \\ \alpha_{k,i2} - \frac{1}{2}e_{k,i2}, & \left|\overline{u}_{k,i}\right| > \Delta_{k,i}, \end{cases} \tag{17}$$

$$\overline{u}_{k,i}(t) = \omega_{k,i}\left(t_{k,i,z}\right), \forall t \in \left[t_{k,i,z}, t_{k,i,z+1}\right), \tag{18}$$

$$\overline{\alpha}_{k,i2} = b_{k,i2}e_{k,i2}^3 + c_{k,i2}e_{k,i2}^{2q-1} + \frac{1}{2\varepsilon_{k,i}^2}\widehat{\vartheta}_{k,i}\left\|S_{k,i}\right\|^2 e_{k,i2} + \widehat{\eta}_{k,i}\tanh\left(\frac{e_{k,i2}}{\tau_{k,i}}\right), \tag{19}$$

where $b_{k,i2}$, $c_{k,i2}$, $\tau_{k,i}$, $\Delta_{k,i}$, $s_{k,i1}$, $s_{k,i2}$, and $\delta_{k,i}$ are positive design constants; $0 < \varrho_{k,i} < 1$, $m_{k,i}(t) = \omega_{k,i}(t) - \overline{u}_{k,i}(t)$; $z \in \mathbb{Z}^+$, $t_{k,i,z+1}$ is the controller update time, and $t_{k,i,1}$ represents the initial time t_0.

Three adaptive laws are established as follows:

$$\dot{\widehat{\zeta}}_{k,i} = \gamma_{k,i}\overline{\alpha}_{k,i2}e_{k,i2} - J_{k,i}\widehat{\zeta}_{k,i} - \frac{J_{k,i}}{\gamma_{k,i}}\widehat{\zeta}_{k,i}^3, \tag{20}$$

$$\dot{\widehat{\eta}}_{k,i} = \sigma_{k,i}e_{k,i2}\tanh\left(\frac{e_{k,i2}}{\tau_{k,i}}\right) - \ell_{k,i}\widehat{\eta}_{k,i} - \frac{\ell_{k,i}}{\sigma_{k,i}}\widehat{\eta}_{k,i}^3, \tag{21}$$

$$\dot{\widehat{\vartheta}}_{k,i} = \frac{1}{2\varepsilon_{k,i}^2}l_{k,i}\left\|S_{k,i}\right\|^2 e_{k,i2}^2 - \flat_{k,i}\widehat{\vartheta}_{k,i} - \frac{\flat_{k,i}}{l_{k,i}}\widehat{\vartheta}_{k,i}^3, \tag{22}$$

where $J_{k,i} > 0$, $\ell_{k,i} > 0$, and $\flat_{k,i} > 0$.

Remark 12. As shown in equation (16), an event is triggered only when the trigger condition is satisfied. Whenever the event is triggered, the control value $\overline{u}_{k,i}(t) = \omega_{k,i}(t_{k,i,k+1})$ will be applied to actuators, and the control value will remain until the next event is triggered. Obviously, this update mechanism of control signals can reduce the update frequency and thus ease the communication pressure.

Then, according to the analysis in the appendix, one has

$$\zeta_{k,i}\overline{u}_{k,i}e_{k,i2} \leq \zeta_{k,i}e_{k,i2}\alpha_{k,i2} + \frac{1}{2}\check{\zeta}_{k,i}s_{k,i1}^2 + \frac{1}{2}\check{\zeta}_{k,i}s_{k,i2}^2 + 0.2785\check{\zeta}_{k,i}\delta_{k,i}. \tag{23}$$

The virtual controller $\alpha_{k,i2}$ is designed as follows:

$$\alpha_{k,i2} = -\frac{e_{k,i2}\widehat{\zeta}_{k,i}^2\overline{\alpha}_{k,i2}^2}{\sqrt{e_{k,i2}^2\widehat{\zeta}_{k,i}^2\overline{\alpha}_{k,i2}^2 + \mu_{k,i}^2}}. \tag{24}$$

From (24), it can be derived that

$$\begin{aligned} \zeta_{k,i}e_{k,i2}\alpha_{k,i2} &= -\frac{\zeta_{k,i}e_{k,i2}^2\hat{\zeta}_{k,i}^2\bar{\alpha}_{k,i2}^2}{\sqrt{e_{k,i2}^2\hat{\zeta}_{k,i}^2\bar{\alpha}_{k,i2}^2 + \mu_{k,i}^2}} \\ &\leq -\underline{\zeta}_{k,i}e_{k,i2}^2\frac{\widehat{\zeta}_{k,i}^2\overline{\alpha}_{k,i2}^2}{\sqrt{e_{k,i2}^2\widehat{\zeta}_{k,i}^2\overline{\alpha}_{k,i2}^2 + \mu_{k,i}^2}} \\ &\leq \underline{\zeta}_{k,i}\mu_{k,i} - \underline{\zeta}_{k,i}\widehat{\zeta}_{k,i}\overline{\alpha}_{k,i2}e_{k,i2}. \end{aligned} \tag{25}$$

It is true that

$$\underline{\zeta}_{k,i}\widehat{\zeta}_{k,i}\overline{\alpha}_{k,i2}e_{k,i2} + \underline{\zeta}_{k,i}\widetilde{\zeta}_{k,i}\overline{\alpha}_{k,i2}e_{k,i2} \geq \overline{\alpha}_{k,i2}e_{k,i2}. \tag{26}$$

Substituting (23), (25), and (26) into (15) gives

$$\begin{aligned} \dot{V}_{k,i2} \leq & -b_{k,i1}e_{k,i1}^4 - c_{k,i1}e_{k,i1}^{2q} - \overline{\alpha}_{k,i2}e_{k,i2} + \overline{\eta}_{k,i}\left|e_{k,i2}\right| + \frac{1}{2\varepsilon_{k,i}^2}\vartheta_{k,i}\left\|S_{k,i}\right\|^2 e_{k,i2}^2 \\ & - \frac{\zeta_{k,i}}{\gamma_{k,i}}\widetilde{\zeta}_{k,i}\left(\dot{\widehat{\zeta}}_{k,i} - \gamma_{k,i}\overline{\alpha}_{k,i2}e_{k,i2}\right) - \frac{1}{\sigma_{k,i}}\widetilde{\eta}_{k,i}\dot{\widehat{\eta}}_{k,i} - \frac{1}{l_{k,i}}\widetilde{\vartheta}_{k,i}\dot{\widehat{\vartheta}}_{k,i} + \underline{\delta}_{k,i}, \end{aligned} \tag{27}$$

where

$$\underline{\delta}_{k,i} = \frac{1}{2}\varepsilon_{k,i}^2 + \frac{1}{2}\overline{v}_{k,i}^2 + \frac{1}{2}\check{\zeta}_{k,i}s_{k,i1}^2 + \frac{1}{2}\check{\zeta}_{k,i}s_{k,i2}^2 + \underline{\zeta}_{k,i}\mu_{k,i} + 0.2785\check{\zeta}_{k,i}\delta_{k,i}. \tag{28}$$

Substituting (19) into (27) gets

$$\dot{V}_{k,i2} \le -\sum_{p=1}^{2} b_{k,ip}e_{k,ip}^4 - \sum_{p=1}^{2} c_{k,ip}e_{k,ip}^{2q} + \bar{\eta}_{k,i}\left|e_{k,i2}\right| - \bar{\eta}_{k,i}e_{k,i2}\tanh\left(\frac{e_{k,i2}}{\tau_{k,i}}\right) - \frac{\zeta_{k,i}\widetilde{\zeta}_{k,i}}{\gamma_{k,i}}\left(\dot{\widehat{\zeta}}_{k,i} - \gamma_{k,i}\bar{\alpha}_{k,i2}e_{k,i2}\right)$$
$$-\frac{1}{\sigma_{k,i}}\widetilde{\eta}_{k,i}\left[\dot{\widehat{\eta}}_{k,i} - \sigma_{k,i}e_{k,i2}\tanh\left(\frac{e_{k,i2}}{\tau_{k,i}}\right)\right] - \frac{1}{l_{k,i}}\widetilde{\vartheta}_{k,i}\left(\dot{\widehat{\vartheta}}_{k,i} - \frac{1}{2\varepsilon_{k,i}^2}l_{k,i}\left\|S_{k,i}\right\|^2 e_{k,i2}^2\right) + \underline{\delta}_{k,i}. \tag{29}$$

Using Lemma 6 and substituting (20)–(22) into (29) gives

$$\begin{aligned}\dot{V}_{k,i2} \le & -\sum_{p=1}^{2} b_{k,ip}e_{k,ip}^4 - \sum_{p=1}^{2} c_{k,ip}e_{k,ip}^{2q} + \frac{\zeta_{k,i}J_{k,i}\widetilde{\zeta}_{k,i}\widehat{\zeta}_{k,i}}{\gamma_{k,i}} + \frac{\zeta_{k,i}J_{k,i}\widetilde{\zeta}_{k,i}\widehat{\zeta}_{k,i}^3}{\gamma_{k,i}^2} + \frac{\ell_{k,i}}{\sigma_{k,i}}\widetilde{\eta}_{k,i}\widehat{\eta}_{k,i} \\ & + \frac{\ell_{k,i}}{\sigma_{k,i}^2}\widetilde{\eta}_{k,i}\widehat{\eta}_{k,i}^3 + \frac{\flat_{k,i}}{l_{k,i}}\widetilde{\vartheta}_{k,i}\widehat{\vartheta}_{k,i} + \frac{\flat_{k,i}}{l_{k,i}^2}\widetilde{\vartheta}_{k,i}\widehat{\vartheta}_{k,i}^3 + \underline{\delta}_{k,i} + 0.2785\overline{\eta}_{k,i}\tau_{k,i}.\end{aligned} \tag{30}$$

Obviously

$$\frac{\zeta_{k,i}J_{k,i}\widetilde{\zeta}_{k,i}\widehat{\zeta}_{k,i}}{\gamma_{k,i}} \le \frac{\zeta_{k,i}J_{k,i}\overline{\zeta}_{k,i}^2}{2\gamma_{k,i}} - \frac{\zeta_{k,i}J_{k,i}\widetilde{\zeta}_{k,i}^2}{2\gamma_{k,i}}. \tag{31}$$

By using Lemma 7 and letting $\epsilon_1 = 1$, $\epsilon_2 = \underline{\zeta}_{k,i}J_{k,i}/2\gamma_{k,i}\widetilde{\zeta}_{k,i}^2$, $\rho_1 = 1 - q$, $\rho_2 = q$, and $k = q^{q/1-q}$, (31) can be written as

$$\frac{\zeta_{k,i}J_{k,i}\widetilde{\zeta}_{k,i}\widehat{\zeta}_{k,i}}{\gamma_{k,i}} \le \frac{\zeta_{k,i}J_{k,i}\overline{\zeta}_{k,i}^2}{2\gamma_{k,i}} - \left(\frac{\zeta_{k,i}J_{k,i}\widetilde{\zeta}_{k,i}^2}{2\gamma_{k,i}}\right)^q + \iota, \tag{32}$$

where $\iota = q^{q/1-q}(1-q)$.

Similar to (31) and (32), one can obtain that

$$\frac{\ell_{k,i}}{\sigma_{k,i}}\widetilde{\eta}_{k,i}\widehat{\eta}_{k,i} \le \frac{\ell_{k,i}}{2\sigma_{k,i}}\overline{\eta}_{k,i}^2 - \left(\frac{\ell_{k,i}}{2\sigma_{k,i}}\widetilde{\eta}_{k,i}^2\right)^q + \iota, \tag{33}$$

$$\frac{\flat_{k,i}}{l_{k,i}}\widetilde{\vartheta}_{k,i}\widehat{\vartheta}_{k,i} \le \frac{\flat_{k,i}}{2l_{k,i}}\vartheta_{k,i}^2 - \left(\frac{\flat_{k,i}}{2l_{k,i}}\widetilde{\vartheta}_{k,i}^2\right)^q + \iota. \tag{34}$$

Substituting (32)–(34) into (30) gives

$$\dot{V}_{k,i2} \le -\sum_{p=1}^{2} b_{k,ip}e_{k,ip}^4 - \sum_{p=1}^{2} c_{k,ip}e_{k,ip}^{2q} - \left(\frac{\zeta_{k,i}J_{k,i}\widetilde{\zeta}_{k,i}^2}{2\gamma_{k,i}}\right)^q + \frac{\zeta_{k,i}J_{k,i}\widetilde{\zeta}_{k,i}\widehat{\zeta}_{k,i}^3}{\gamma_{k,i}^2}$$
$$-\left(\frac{\ell_{k,i}}{2\sigma_{k,i}}\widetilde{\eta}_{k,i}^2\right)^q + \frac{\ell_{k,i}}{\sigma_{k,i}^2}\widetilde{\eta}_{k,i}\widehat{\eta}_{k,i}^3 - \left(\frac{\flat_{k,i}}{2l_{k,i}}\widetilde{\vartheta}_{k,i}^2\right)^q + \frac{\flat_{k,i}}{l_{k,i}^2}\widetilde{\vartheta}_{k,i}\widehat{\vartheta}_{k,i}^3 + \check{\delta}_{k,i}, \tag{35}$$

where

$$\breve{\delta}_{k,i} = \underline{\delta}_{k,i} + 0.2785\overline{\eta}_{k,i}\tau_{k,i} + \frac{\zeta_{k,i}J_{k,i}\overline{\zeta}_{k,i}^2}{2\gamma_{k,i}} + \frac{\ell_{k,i}}{2\sigma_{k,i}}\overline{\eta}_{k,i}^2 + \frac{\flat_{k,i}}{2l_{k,i}}\vartheta_{k,i}^2 + 3\iota. \tag{36}$$

According to the definition of $\widetilde{\zeta}_{k,i}$, one has

$$\widetilde{\zeta}_{k,i}\widetilde{\zeta}_{k,i}^3 = \widetilde{\zeta}_{k,i}\left(\overline{\zeta}_{k,i}^3 + 3\overline{\zeta}_{k,i}\widetilde{\zeta}_{k,i}^2 - 3\overline{\zeta}_{k,i}^2\widetilde{\zeta}_{k,i} - \widetilde{\zeta}_{k,i}^3\right). \tag{37}$$

Using Young's inequality, we have

$$\widetilde{\zeta}_{k,i}\overline{\zeta}_{k,i}^3 \le \frac{\overline{\zeta}_{k,i}^4}{12} + 3\overline{\zeta}_{k,i}^2\widetilde{\zeta}_{k,i}^2, \tag{38}$$

$$3\widetilde{\zeta}_{k,i}^3\overline{\zeta}_{k,i} \le \frac{9\pi_{k,i}^{4/3}\widetilde{\zeta}_{k,i}^4}{4} + \frac{3\overline{\zeta}_{k,i}^4}{4\pi_{k,i}^4}, \tag{39}$$

where $\pi_{k,i} > 0$.

Combining (37)–(39) yields

$$\frac{\zeta_{k,i}J_{k,i}}{\gamma_{k,i}^2}\widetilde{\zeta}_{k,i}\widetilde{\zeta}_{k,i}^3 \le -\left(4\underline{\zeta}_{k,i}J_{k,i} - 9\underline{\zeta}_{k,i}J_{k,i}\pi_{k,i}^{4/3}\right)\left(\frac{1}{2\gamma_{k,i}}\widetilde{\zeta}_{k,i}^2\right)^2 + \frac{\zeta_{k,i}J_{k,i}\overline{\zeta}_{k,i}^4}{12\gamma_{k,i}^2} + \frac{3\underline{\zeta}_{k,i}J_{k,i}\overline{\zeta}_{k,i}^4}{4\gamma_{k,i}^2\pi_{k,i}^4}. \tag{40}$$

Similar to (37)–(40), one can obtain that

$$\frac{\ell_{k,i}}{\sigma_{k,i}^2}\widetilde{\eta}_{k,i}\widetilde{\eta}_{k,i}^3 \le -\left(4\ell_{k,i} - 9\ell_{k,i}\pi_{k,i}^{4/3}\right)\left(\frac{1}{2\sigma_{k,i}}\widetilde{\eta}_{k,i}^2\right)^2 + \frac{\ell_{k,i}\overline{\eta}_{k,i}^4}{12\sigma_{k,i}^2} + \frac{3\ell_{k,i}\overline{\eta}_{k,i}^4}{4\sigma_{k,i}^2\pi_{k,i}^4}, \tag{41}$$

$$\frac{\flat_{k,i}}{l_{k,i}^2}\widetilde{\vartheta}_{k,i}\widetilde{\vartheta}_{k,i}^3 \le -\left(4\flat_{k,i} - 9\flat_{k,i}\pi_{k,i}^{4/3}\right)\left(\frac{1}{2l_{k,i}}\widetilde{\vartheta}_{k,i}^2\right)^2 + \frac{\flat_{k,i}\vartheta_{k,i}^4}{12l_{k,i}^2} + \frac{3\flat_{k,i}\vartheta_{k,i}^4}{4l_{k,i}^2\pi_{k,i}^4}. \tag{42}$$

Substituting (40)–(42) into (35) yields

$$\begin{aligned}\dot{V}_{k,i2} \le & -\sum_{p=1}^{2} b_{k,ip}e_{k,ip}^4 - \sum_{p=1}^{2} c_{k,ip}e_{k,ip}^{2q} - \left(\frac{\zeta_{k,i}J_{k,i}}{2\gamma_{k,i}}\widetilde{\zeta}_{k,i}^2\right)^q - \left(4\underline{\zeta}_{k,i}J_{k,i} - 9\underline{\zeta}_{k,i}J_{k,i}\pi_{k,i}^{4/3}\right)\left(\frac{1}{2\gamma_{k,i}}\widetilde{\zeta}_{k,i}^2\right)^2 \\ & - \left(\frac{\ell_{k,i}}{2\sigma_{k,i}}\widetilde{\eta}_{k,i}^2\right)^q - \left(4\ell_{k,i} - 9\ell_{k,i}\pi_{k,i}^{4/3}\right)\left(\frac{1}{2\sigma_{k,i}}\widetilde{\eta}_{k,i}^2\right)^2 - \left(\frac{\flat_{k,i}}{2l_{k,i}}\widetilde{\vartheta}_{k,i}^2\right)^q - \left(4\flat_{k,i} - 9\flat_{k,i}\pi_{k,i}^{4/3}\right)\left(\frac{1}{2l_{k,i}}\widetilde{\vartheta}_{k,i}^2\right)^2 + \breve{\delta}_{k,i},\end{aligned} \tag{43}$$

where

$$\breve{\delta}_{k,i} = \breve{\delta}_{k,i} + \frac{\zeta_{k,i}J_{k,i}\overline{\zeta}_{k,i}^4}{12\gamma_{k,i}^2} + \frac{3\underline{\zeta}_{k,i}J_{k,i}\overline{\zeta}_{k,i}^4}{4\gamma_{k,i}^2\pi_{k,i}^4} + \frac{\ell_{k,i}\overline{\eta}_{k,i}^4}{12\sigma_{k,i}^2} + \frac{3\ell_{k,i}\overline{\eta}_{k,i}^4}{4\sigma_{k,i}^2\pi_{k,i}^4} + \frac{\flat_{k,i}\vartheta_{k,i}^4}{12l_{k,i}^2} + \frac{3\flat_{k,i}\vartheta_{k,i}^4}{4l_{k,i}^2\pi_{k,i}^4}. \tag{44}$$

Using Lemma 8, one has

$$\dot{V}_{k,i2} \leq -\psi_{k,i1}\left(\sum_{p=1}^{2}\frac{1}{2}e_{k,ip}^2\right)^q - \phi_{k,i1}\left(\sum_{p=1}^{2}\frac{1}{2}e_{k,ip}^2\right)^2 - \psi_{k,i2}\left(\frac{\zeta_{k,i}}{2\gamma_{k,i}}\tilde{\zeta}_{k,i}^2\right)^q - \phi_{k,i2}\left(\frac{\zeta_{k,i}}{2\gamma_{k,i}}\tilde{\zeta}_{k,i}^2\right)^2 - \psi_{k,i3}\left(\frac{1}{2\sigma_{k,i}}\tilde{\eta}_{k,i}^2\right)^q - \phi_{k,i3}\left(\frac{1}{2\sigma_{k,i}}\tilde{\eta}_{k,i}^2\right)^2 - \psi_{k,i4}\left(\frac{1}{2l_{k,i}}\tilde{\vartheta}_{k,i}^2\right)^q - \phi_{k,i4}\left(\frac{1}{2l_{k,i}}\tilde{\vartheta}_{k,i}^2\right)^2 + \breve{\delta}_{k,i}, \tag{45}$$

where $\psi_{k,i1} = 2^q \min\{c_{k,i1}, c_{k,i2}\}$, $\phi_{k,i1} = 2\min\{b_{k,i1}, b_{k,i2}\}$, $\psi_{k,i2} = j_{k,i}^q$, $\phi_{k,i2} = 4J_{k,i} - 9J_{k,i}\pi_{k,i}^{4/3}/\underline{\zeta}_{k,i}$, $\psi_{k,i3} = \ell_{k,i}^q$, $\phi_{k,i3} = 4\ell_{k,i} - 9\ell_{k,i}\pi_{k,i}^{4/3}$, $\psi_{k,i4} = \flat_{k,i}^q$, and $\phi_{k,i4} = 4\flat_{k,i} - 9\flat_{k,i}\pi_{k,i}^{4/3}$.

Ultimately, we can get

$$\dot{V}_{k,i2} \leq -\psi_{k,i}V_{k,i2}^q - \phi_{k,i}V_{k,i2}^2 + \breve{\delta}_{k,i}, \tag{46}$$

where $\psi_{k,i} = \min\{\psi_{k,i1}, \psi_{k,i2}, \psi_{k,i3}, \psi_{k,i4}\}$ and $\phi_{k,i} = \min\{\phi_{k,i1}, \phi_{k,i2}, \phi_{k,i3}, \phi_{k,i4}\}/4$.

3.2. Stability Analysis

Theorem 13. *Considering the MASs (3) under Assumptions 2–4, the distributed event-triggered controller (18) can guarantee that*

(1) All the closed-loop signals are bounded, and the output of each follower can track the output of the leader within a fixed time;

(2) The Zeno behavior is avoided.

Proof. According to Lemma 6 in [38], the error signals $\aleph_{k,i} = [e_{k,i1}, e_{k,i2}, \tilde{\vartheta}_{k,i}, \tilde{\zeta}_{k,i}, \tilde{\eta}_{k,i}]^T$ can converge to the following residue set:

$$\Theta_{k,i} = \left\{\aleph_{k,i} \,\middle|\, V_{k,i2}(\aleph_{k,i}) \leq \min\left\{\left(\frac{\breve{\delta}_{k,i}}{(1-\theta)\psi_{k,i}}\right)^{1/q}, \left(\frac{\breve{\delta}_{k,i}}{(1-\theta)\phi_{k,i}}\right)^{1/2}\right\}\right\}, \tag{47}$$

$$T_{k,i} \leq \frac{1}{\psi\theta(1-q)} + \frac{1}{\phi\theta(q-1)}. \tag{48}$$

Thus, the error signals $\aleph_{k,i}$ can converge to the set given by (47) after the fixed time $T_{k,i}$. Then, according to inequality (47), we can easily obtain that $x_{k,i1}$, $x_{k,i2}$, $\hat{\vartheta}_{k,i}$, $\hat{\zeta}_{k,i}$, $\hat{\eta}_{k,i}$, $\alpha_{k,i1}$, $\alpha_{k,i2}$, $\omega_{k,i}$, $\overline{u}_{k,i}$, and $u_{k,i}$ are bounded.

We define the synchronization error vector as $E_i = [e_{1,i1}, e_{2,i1}, \ldots, e_{N,i1}]^T$. Then, according to [8], one has

$$\|\overline{E}_i\| \leq \frac{\|E_i\|}{\lambda_{\max}(\mathscr{L} + \mathscr{H})}, \tag{49}$$

where $\lambda_{\max}(\mathscr{L} + \mathscr{H})$ is the maximum eigenvalue of the matrix $\mathscr{L} + \mathscr{H}$; $\overline{E}_i = [\overline{e}_{1,i}, \overline{e}_{2,i}, \ldots, \overline{e}_{N,i}]^T = Y_i - \overline{Y}_i$, $Y_i = [y_{1,i}, y_{2,i}, \ldots, y_{N,i}]^T$, $\overline{Y}_i = [\overbrace{y_{0,i}, \ldots y_{0,i}}^{N}]^T$. Therefore, the tracking error $\overline{e}_{k,i}$ can converge to the set given by

$$|\overline{e}_{k,i}| \leq \min\left\{\frac{\sqrt{2}}{\lambda_{\max}(\mathscr{L} + \mathscr{H})}\left(\frac{\breve{\delta}_{k,i}}{(1-\theta)\psi_{k,i}}\right)^{1/2q}, \frac{\sqrt{2}}{\lambda_{\max}(\mathscr{L} + \mathscr{H})}\left(\frac{\breve{\delta}_{k,i}}{(1-\theta)\phi_{k,i}}\right)^{1/4}\right\}. \tag{50}$$

As $\omega_{k,i}$ is a function about $\alpha_{k,i2}$ and $e_{k,i2}$, we can obtain $\dot{\omega}_{k,i}$ is bounded, *i.e.*, $\dot{\omega}_{k,i} \leq \overline{\omega}_{k,i}$ with $\overline{\omega}_{k,i} > 0$. In addition, when $|\overline{u}_{k,i}| \leq \Delta_{k,i}$, $\lim_{t \longrightarrow t_{k,i,z+1}} m_{k,i}(t) = s_{k,i1} + \varrho_{k,i}|\overline{u}_{k,i}(t)|$, $m_{k,i}(t_{k,i,z}) = 0$, so the time interval satisfies $t_{k,i}^* \geq s_{k,i1} + \varrho_{k,i}|\overline{u}_{k,i}(t)|/\overline{\omega}_{k,i}$. Similarly, when $|\overline{u}_{k,i}| > \Delta_{k,i}$, one has $t_{k,i}^* \geq s_{k,i1}/\overline{\omega}_{k,i}$. Obviously, the Zeno behavior is successfully avoided. □

Remark 14. The fixed-time stability can be obtained by selecting the appropriate design parameters, and the tracking error can converge to near the origin within a fixed period of time $T_{k,i}$. It is worth mentioning that the time $T_{k,i}$ is independent of the initial system states, which is an advantage of fixed-time stability. This property will be demonstrated in simulation experiments.

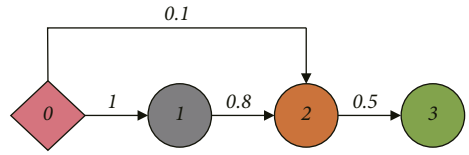

Figure 1: The directed communication graph.

4. Simulations and Results

The suggested algorithm is deployed to a collection of autonomous surface vessels (ASVs) in order to test its efficacy. Figure 1 expresses the communication topology between ASVs (0 represents the leader; 1, 2, and 3 represent the followers), and the model of ASV (see [39]) is described by

$$\begin{cases} \dot{x}_{k,1} = x_{k,2}, \\ g_k(t)\dot{x}_{k,2} = \rho_k(t)\overline{u}_k + r_k(t) + f_k\left(x_{k,1}, x_{k,2}\right) + d_k(t), \\ y_k = x_{k,1}, \end{cases} \tag{51}$$

where $x_{k,1} = [x_{k,11}, x_{k,21}, x_{k,31}]^T$ and $x_{k,2} = [x_{k,12}, x_{k,22}, x_{k,32}]^T$ represent the position and velocity, respectively; $g_k(t) = diag\{g_{k,1}, g_{k,2}, g_{k,3}\}$ is the mass matrix. $d_k = [d_{k,1}, d_{k,2}, d_{k,3}]^T$ is an unknown external disturbance; $\overline{u}_k = [\overline{u}_{k,1}, \overline{u}_{k,2}, \overline{u}_{k,3}]^T$ and $y_k = [y_{k,1}, y_{k,2}, y_{k,3}]^T$ represent the control input and output of agent k, respectively. f_k represents centripetal, Coriolis, and hydrodynamic damping forces and torques, where $f_k = \Xi \cdot x_{k,2}$ with

$$\Xi = \begin{bmatrix} A + \underline{A}\left|x_{k,12}\right| & -g_{k,2}x_{k,32} & 0 \\ g_{k,1}x_{k,32} & B + \underline{B}\left|x_{k,22}\right| & 0 \\ 0 & 0 & C + \underline{C}\left|x_{k,32}\right| \end{bmatrix}. \tag{52}$$

The physical parameters are given as follows: $g_{k,1} = 500 + 5\sin(1/10t)$, $g_{k,2} = 1000 + 10\sin(1/10t)$, $g_{k,3} = 800 + 8\sin(1/10t)$, $A = -1 + 0.1(-1)^k$, $\underline{A} = -25 + 2.5(-1)^k$, $B = -10 + (-1)^k$, $\underline{B} = -200 + 20(-1)^k$, $C = -0.5 + 0.05(-1)^k$, $\underline{C} = -1500 + 150(-1)^k$, $d_{k,1} = 3 - 0.1(-1)^k \sin(1/50t)$, $d_{k,2} = 3 - 0.2(-1)^k \sin(1/50t)$, and $d_{k,3} = 3 - 0.1(-1)^k \sin(1/50t)$ for $k = 1, 2, 3$.

The initial states of the system is given as follows: $x_{1,1}(0) = [0.3, 0.3, 0.3]^T$, $x_{2,1}(0) = [0.2, 0.2, 0.2]^T$, $x_{3,1}(0) = [0.1, 0.1, 0.1]^T$, $x_{1,2}(0) = [0, 0, 0]^T$, $x_{2,2}(0) = [0, 0, 0]^T$, and $x_{3,2}(0) = [0, 0, 0]^T$. Assume that the output of the leader is $y_0 = [\sin(2t), \sin(2t), 0]^T$.

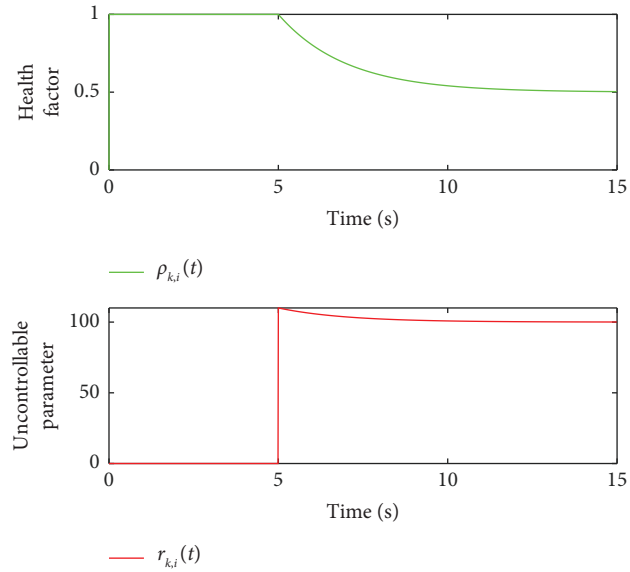

Figure 2: The parameters of actuator failures.

In the simulation experiment, the failure of the actuator is considered and the failure model is $u_k = \rho_k(t)\overline{u}_k + r_k(t)$ with $\rho_k(t) = \text{diag}\{\rho_{k,1}(t), \rho_{k,2}(t), \rho_{k,3}(t)\}$ and $r_k(t) = [r_{k,1}(t), r_{k,2}(t), r_{k,3}(t)]^T$ where

$$\begin{aligned} \rho_{k,i}(t) &= \begin{cases} 1, & t < 5s, \\ 0.5 + 0.5e^{-0.5(t-5)}, & t \geq 5s, \end{cases} \\ r_{k,i}(t) &= \begin{cases} 0, & t < 5s, \\ 100 + 10e^{-0.5(t-5)}, & t \geq 5s. \end{cases} \end{aligned} \tag{53}$$

Furthermore, to better demonstrate the actuator operation, Figure 2 is provided. As shown in Figure 2, the actuator works normally until 5 s and then starts to fail.

The distributed controller is designed as follows:

Table 1: Part 1 of design parameters of the controller.

Followers	Parameters													
	$b_{k,11}$	$b_{k,21}$	$b_{k,31}$	$c_{k,11}$	$c_{k,21}$	$c_{k,31}$	$b_{k,12}$	$b_{k,22}$	$b_{k,32}$	$c_{k,12}$	$c_{k,22}$	$c_{k,32}$	$\mu_{k,i}$	$\delta_{k,i}$
1	5	5	5	5	5	5	150	150	100	150	150	100	0.01	0.2
2	7	7	7	7	7	7	200	200	150	200	200	150	0.01	0.4
3	8	8	5	8	8	5	250	250	100	250	250	100	0.01	0.4

Table 2: Part 2 of design parameters of the controller.

Followers	Parameters													
	$\varrho_{k,i}$	$s_{k,i1}$	$s_{k,i2}$	$\Delta_{k,1}$	$\Delta_{k,2}$	$\Delta_{k,3}$	$l_{k,i}$	$\varepsilon_{k,i}$	$\flat_{k,i}$	$\sigma_{k,i}$	$\tau_{k,i}$	$\ell_{k,i}$	$\gamma_{k,i}$	$J_{k,i}$
1	1000	1000	2000	5000	5000	0.5	0.5	0.1	0.1	1	0.1	0.1	1	0.001
2	2000	3000	2000	5000	5000	0.5	0.5	0.1	0.1	1	0.1	0.1	1	0.001
3	2000	3000	2000	5000	5000	0.5	0.5	0.1	0.1	1	0.1	0.1	1	0.001

$$
\begin{aligned}
\alpha_{k,i1} &= \frac{1}{h_k + d_k}\left(-b_{k,i1}e_{k,i1}^3 - c_{k,i1}e_{k,i1}^{2q-1} + \sum_{j\in\mathcal{N}_k} a_{kj}x_{j,i2} + h_k\dot{y}_{0,i}\right),\\
t_{k,i,z+1} &= \begin{cases} \inf\left\{t \in \mathbb{R} \mid \left|m_{k,i}(t)\right| \geq s_{k,i1} + \varrho_{k,i}\left|\overline{u}_{k,i}(t)\right|\right\}, \left|\overline{u}_{k,i}\right| \leq \Delta_{k,i},\\ \inf\left\{t \in \mathbb{R} \mid \left|m_{k,i}(t)\right| \geq s_{k,i2}\right\}, \left|\overline{u}_{k,i}\right| > \Delta_{k,i}, \end{cases}\\
\omega_{k,i}(t) &= \begin{cases} -\alpha_{k,i2}\tanh\left(\dfrac{e_{k,i2}\alpha_{k,i2}}{\delta_{k,i}}\right)\left(1+\varrho_{k,i}\right) - \dfrac{\left(1+\varrho_{k,i}\right)e_{k,i2}}{2\left(1-\varrho_{k,i}\right)^2}, \left|\overline{u}_{k,i}\right| \leq \Delta_{k,i},\\ \alpha_{k,i2} - \dfrac{1}{2}e_{k,i2}, \left|\overline{u}_{k,i}\right| > \Delta_{k,i}, \end{cases}\\
\overline{u}_{k,i}(t) &= \omega_{k,i}\left(t_{k,i,z}\right), \forall t \in \left[t_{k,i,z}, t_{k,i,z+1}\right),
\end{aligned}
\tag{54}
$$

$$
\begin{aligned}
\alpha_{k,i2} &= -\frac{e_{k,i2}\widehat{\zeta}_{k,i}^2\overline{\alpha}_{k,i2}^2}{\sqrt{e_{k,i2}^2\widehat{\zeta}_{k,i}^2\overline{\alpha}_{k,i2}^2 + \mu_{k,i}^2}},\\
\overline{\alpha}_{k,i2} &= b_{k,i2}e_{k,i2}^3 + c_{k,i2}e_{k,i2}^{2q-1} + \frac{1}{2\varepsilon_{k,i}^2}\widehat{\vartheta}_{k,i}\left\|S_{k,i}\right\|^2 e_{k,i2} + \widehat{\eta}_{k,i}\tanh\left(\frac{e_{k,i2}}{\tau_{k,i}}\right),\\
\dot{\widehat{\zeta}}_{k,i} &= \gamma_{k,i}\overline{\alpha}_{k,i2}e_{k,i2} - J_{k,i}\widehat{\zeta}_{k,i} - \frac{J_{k,i}}{\gamma_{k,i}}\widehat{\zeta}_{k,i}^3,\\
\dot{\widehat{\eta}}_{k,i} &= \sigma_{k,i}e_{k,i2}\tanh\left(\frac{e_{k,i2}}{\tau_{k,i}}\right) - \ell_{k,i}\widehat{\eta}_{k,i} - \frac{\ell_{k,i}}{\sigma_{k,i}}\widehat{\eta}_{k,i}^3,\\
\dot{\widehat{\vartheta}}_{k,i} &= \frac{1}{2\varepsilon_{k,i}^2}l_{k,i}\left\|S_{k,i}\right\|^2 e_{k,i2}^2 - \flat_{k,i}\widehat{\vartheta}_{k,i} - \frac{\flat_{k,i}}{l_{k,i}}\widehat{\vartheta}_{k,i}^3,
\end{aligned}
\tag{55}
$$

where $k = 1, 2, 3$, $i = 1, 2, 3$, $q = 4/5$, and the relevant design parameters are given in Tables 1 and 2. The initial values of the adaptive parameters are $\widehat{\vartheta}(0) = 0$, $\widehat{\eta}(0) = 0$ and $\widehat{\zeta}(0) = 0$.

The simulation results are given in Figures 3–5 and Table 3, and it is clear that all signals are bounded. The output trajectories and synchronization errors of each follower are described in Figure 3. Even if the system is affected by actuator failures, the output of the followers is aligned with that of the leader. Time intervals for triggering events are shown in Figure 4, and obviously no Zeno phenomenon

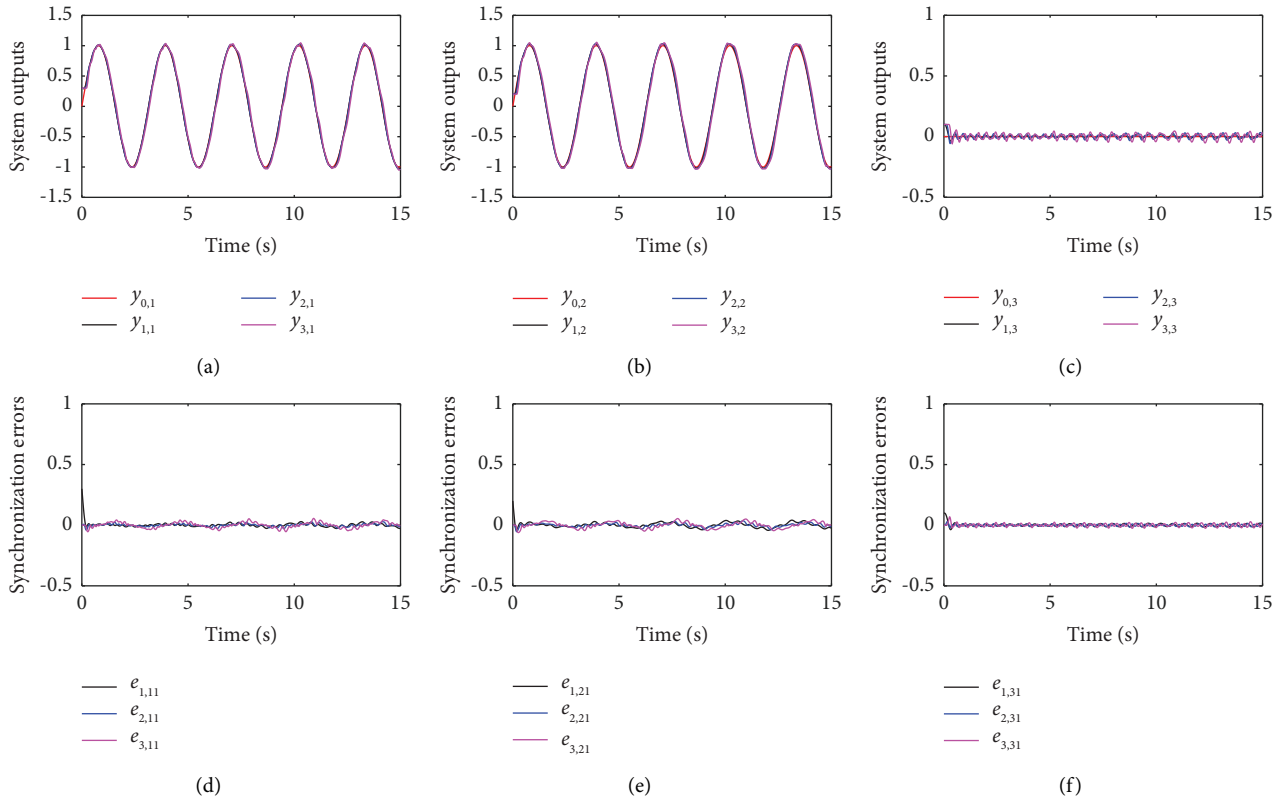

FIGURE 3: System outputs and synchronization errors. (a) System outputs. (b) System outputs. (c) System outputs. (d) Synchronization errors. (e) Synchronization errors. (f) Synchronization errors.

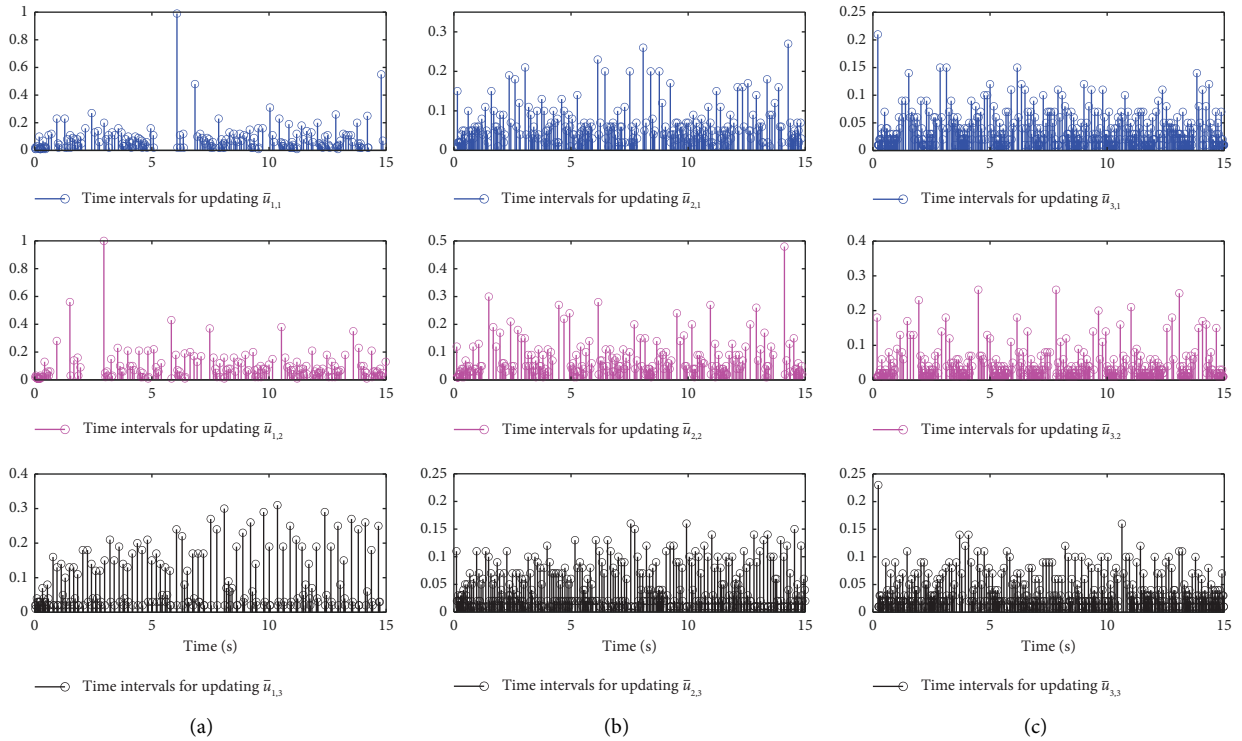

FIGURE 4: Time intervals for updating $u_{k,i}$ $(k = 1, 2, 3; i = 1, 2, 3)$. (a) $t_{1,i,z+1} - t_{1,i,z}$. (b) $t_{2,i,z+1} - t_{2,i,z}$. (c) $t_{3,i,z+1} - t_{3,i,z}$.

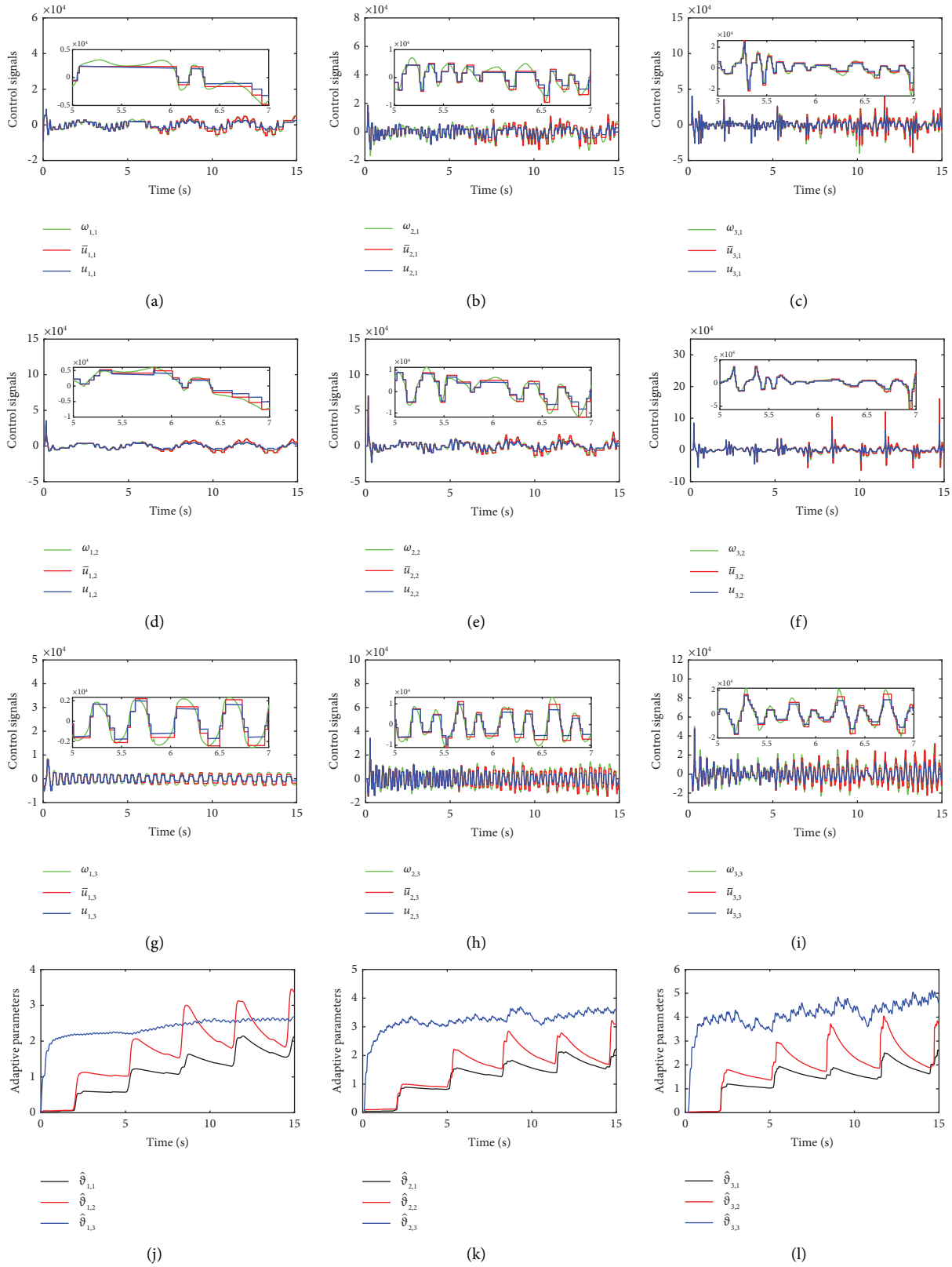

Figure 5: Continued.

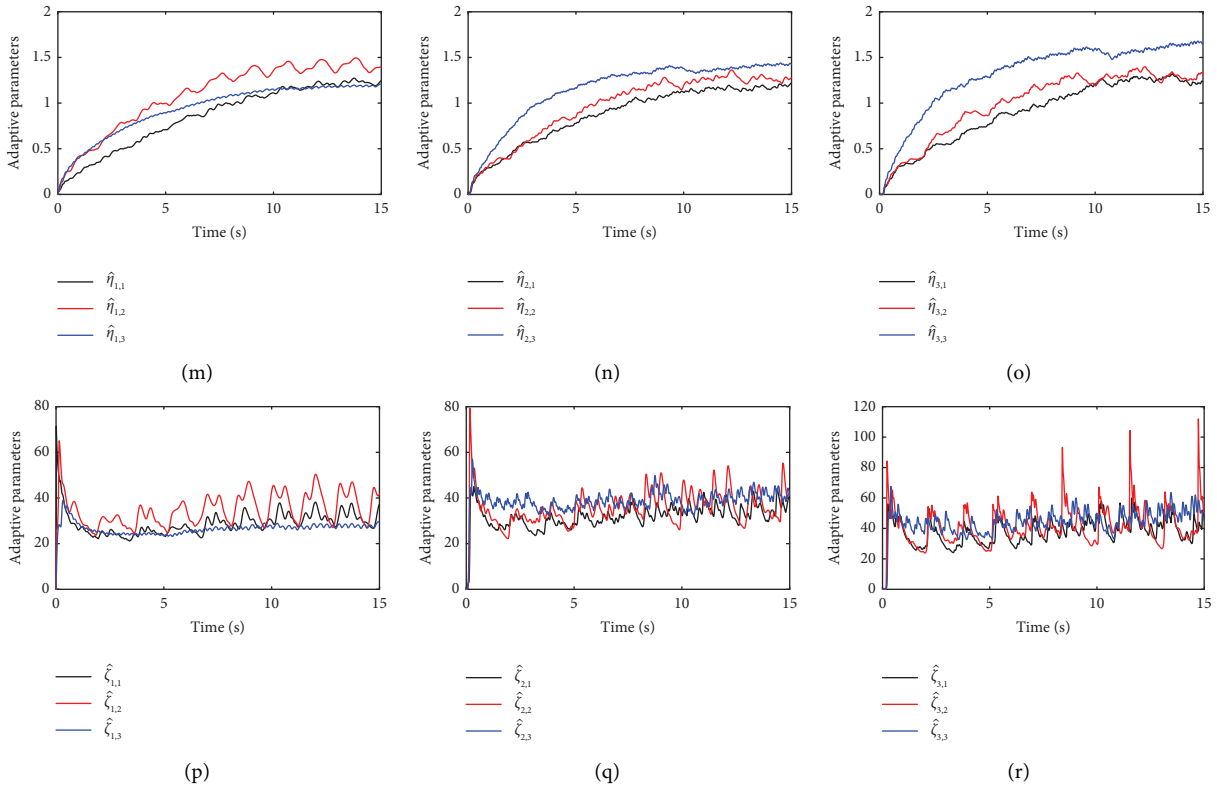

FIGURE 5: The curves of control signals and adaptive parameters. (a) $\omega_{1,1}$, $\overline{u}_{1,1}$, and $u_{1,1}$. (b) $\omega_{2,1}$, $\overline{u}_{2,1}$, and $u_{2,1}$. (c) $\omega_{3,1}$, $\overline{u}_{3,1}$, and $u_{3,1}$. (d) $\omega_{1,2}$, $\overline{u}_{1,2}$, and $u_{1,2}$. (e) $\omega_{2,2}$, $\overline{u}_{2,2}$, and $u_{2,2}$. (f) $\omega_{3,2}$, $\overline{u}_{3,2}$, and $u_{3,2}$. (g) $\omega_{1,3}$, $\overline{u}_{1,3}$, and $u_{1,3}$. (h) $\omega_{2,3}$, $\overline{u}_{2,3}$, and $u_{2,3}$. (i) $\omega_{3,3}$, $\overline{u}_{3,3}$, and $u_{3,3}$. (j) $\vartheta_{1,1}$, $\vartheta_{1,2}$, and $\vartheta_{1,3}$. (k) $\vartheta_{2,1}$, $\vartheta_{2,2}$, and $\vartheta_{2,3}$. (l) $\vartheta_{3,1}$, $\vartheta_{3,2}$, and $\vartheta_{3,3}$. (m) $\eta_{1,1}$, $\eta_{1,2}$, and $\eta_{1,3}$. (n) $\eta_{2,1}$, $\eta_{2,2}$, and $\eta_{2,3}$. (o) $\eta_{3,1}$, $\eta_{3,2}$, and $\eta_{3,3}$. (p) $\zeta_{1,1}$, $\zeta_{1,2}$, and $\zeta_{1,3}$. (q) $\zeta_{2,1}$, $\zeta_{2,2}$, and $\zeta_{2,3}$. (r) $\zeta_{3,1}$, $\zeta_{3,2}$, and $\zeta_{3,3}$.

TABLE 3: The detailed trigger data.

Control inputs	Trigger counts (times)					
	0–3 s	3–6 s	6–9 s	9–12 s	13–15 s	0–15 s
$\overline{u}_{1,1}$	46	30	36	37	36	185
$\overline{u}_{1,2}$	35	30	30	35	37	167
$\overline{u}_{1,3}$	57	32	34	32	30	185
$\overline{u}_{2,1}$	50	53	43	61	41	248
$\overline{u}_{2,2}$	47	43	47	44	36	217
$\overline{u}_{2,3}$	92	77	73	69	74	385
$\overline{u}_{3,1}$	90	80	77	107	95	449
$\overline{u}_{3,2}$	77	87	88	87	77	416
$\overline{u}_{3,3}$	90	69	95	84	100	438

appears. As can be seen in Figures 5(a)–5(i), actuators start to fail after 5 s of operation. In Figures 5(j)–5(r), the dynamics of the adaptive parameters demonstrate the validity of the adaptive laws. To demonstrate that the proposed method can save communication resources, detailed trigger data are recorded in Table 3. In the simulation experiment, the sampling time is 0.01 s, which means that the system needs to update the control signal $\overline{u}_{k,i}(i,k=1,2,3)$ 1500 times for 15 s of operation. Thus, it can be concluded from Table 3 that the proposed method saves a significant amount of communication resources. In addition, to demonstrate that the upper bound of convergence time is independent of the system's initial states, Figure 6 provides the convergence curves of $e_{1,11}$ for different initial states. The

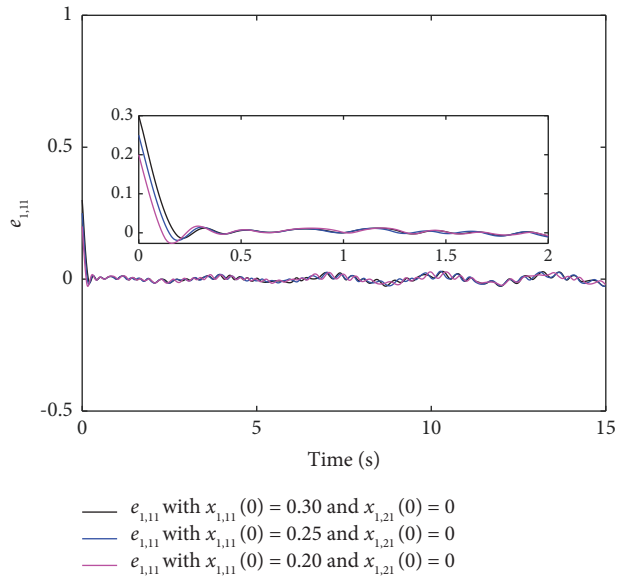

Figure 6: The synchronization error $e_{1,11}$ with different initial system states.

simulation result shows that the convergence time in various initial states is approximately 0.25 s, which demonstrates the fixed-time stability.

5. Conclusions

In this study, a fixed-time consensus control method has been developed for uncertain nonlinear MASs with actuator failures. To achieve the adaptive compensation for actuator failures, unknown control gains, and external disturbances, a boundary estimation method is presented. Furthermore, considering that the implementation of this boundary estimation method requires lots of communication resources, an event triggering mechanism is designed to reduce the update frequency of the controller. It is demonstrated from theory and experiments that by using the suggested method, all signals of the closed-loop system are bounded, and the tracking error of the system can converge to a set near the origin in a fixed time while saving a lot of communication resources. The proposed method requires all state information of the system, but in engineering applications, the system states may be unmeasurable. Based on this research, we will examine the output feedback consensus control in the future.

Appendix

The calculation of $\zeta_{k,i}\overline{u}_{k,i}e_{k,i2}$ in (15) can be divided into two cases.

Case 15. $|\overline{u}_{k,i}| \le \Delta_{k,i}$. According to (16) and (17), $|m_{k,i}(t)| < s_{k,i1} + \varrho_{k,i}|\overline{u}_{k,i}(t)|$ holds for $\forall t \in [t_{k,i,z}, t_{k,i,z+1})$. Furthermore, one can obtain $\overline{u}_{k,i}(t) = \omega_{k,i}(t) - s_{k,i1}\beta_{k,i1}(t)/1 + \varrho_{k,i}\beta_{k,i2}(t)$ with $|\beta_{k,i1}(t)| \le 1$ and $|\beta_{k,i2}(t)| \le 1$. Therefore, we can obtain

$$\zeta_{k,i}\overline{u}_{k,i}e_{k,i2} = -\zeta_{k,i}e_{k,i2}\left\{\frac{1+\varrho_{k,i}}{1+\varrho_{k,i}\beta_{k,i2}(t)}\left[\alpha_{k,i2}\tanh\left(\frac{e_{k,i2}\alpha_{k,i2}}{\delta_{k,i}}\right)\right] + \frac{\left(1+\varrho_{k,i}\right)e_{k,i2}}{2\left(1+\varrho_{k,i}\beta_{k,i2}(t)\right)\left(1-\varrho_{k,i}\right)^2} + \frac{s_{k,i1}\beta_{k,i1}(t)}{1+\varrho_{k,i}\beta_{k,i2}(t)}\right\}. \tag{A.1}$$

Using Lemma 6, (A.1) can be rewritten as

$$\begin{aligned}\zeta_{k,i}\overline{u}_{k,i}e_{k,i2} &\le \zeta_{k,i}\left(\left|e_{k,i2}\alpha_{k,i2}\right| - e_{k,i2}\alpha_{k,i2}\tanh\left(\frac{e_{k,i2}\alpha_{k,i2}}{\delta_{k,i}}\right) - \left|e_{k,i2}\alpha_{k,i2}\right| - \frac{e_{k,i2}^2}{2\left(1-\varrho_{k,i}\right)^2} + \left|\frac{s_{k,i1}e_{k,i2}}{1-\varrho_{k,i}}\right|\right)\\ &\le \zeta_{k,i}e_{k,i2}\alpha_{k,i2} + \frac{1}{2}\check{\zeta}_{k,i}s_{k,i1}^2 + 0.2785\check{\zeta}_{k,i}\delta_{k,i}.\end{aligned} \tag{A.2}$$

where $\check{\zeta}_{k,i} = \sup_{t\geq 0}\{\zeta_{k,i}\} > 0$.

Case 16. $|\overline{u}_{k,i}| > \Delta_{k,i}$. Similarly, for $\forall t \in [t_{k,i,z}, t_{k,i,z+1})$, one can obtain that $\overline{u}_{k,i}(t) = \omega_{k,i}(t) - s_{k,i2}\beta_{k,i1}(t)$ with $|\beta_{k,i1}(t)| \leq 1$. Thus, it can be obtained that

$$\begin{aligned}\zeta_{k,i}\overline{u}_{k,i}e_{k,i2} &\leq \zeta_{k,i}\left(e_{k,i2}\alpha_{k,i2} - \frac{1}{2}e_{k,i2}^2 + \left|s_{k,i2}e_{k,i2}\right|\right)\\ &\leq \zeta_{k,i}e_{k,i2}\alpha_{k,i2} + \frac{1}{2}\check{\zeta}_{k,i}s_{k,i2}^2.\end{aligned} \tag{A.3}$$

Combining Cases 15 and 16 yields

$$\zeta_{k,i}\overline{u}_{k,i}e_{k,i2} \leq \zeta_{k,i}e_{k,i2}\alpha_{k,i2} + \frac{1}{2}\check{\zeta}_{k,i}s_{k,i1}^2 + \frac{1}{2}\check{\zeta}_{k,i}s_{k,i2}^2 + 0.2785\check{\zeta}_{k,i}\delta_{k,i}. \tag{A.4}$$

Data Availability

No data were used to support the findings of this study.

Conflicts of Interest

The authors declare that they have no conflicts of interest.

Authors' Contributions

Jianhui Wang performed conceptualization, methodology, writing of the original draft, and writing of the review. Chen Wang conducted methodology, validation, formal analysis, and writing of the original draft. Kairui Chen performed supervision, resources, funding acquisition, and project administration. Zitao Chen conducted investigation, validation, and data curation.

Acknowledgments

This work is supported by National Natural Science Foundation of China (Grant no. 62103115), the Natural Science Foundation of Guangdong Province (Grant no. 2021A1515011636), the Project of Guangzhou University (Grant no. RC2023007), and the Guangzhou Yangcheng Scholars Research Project (Grant no. 202235199).

References

[1] P. Shi and B. Yan, "A survey on intelligent control for multiagent systems," *IEEE Transactions on Systems, Man, and Cybernetics: Systems*, vol. 51, no. 1, pp. 161–175, 2021.

[2] L. Cao, Y. Pan, H. Liang, and T. Huang, "Observer-based dynamic event-triggered control for multiagent systems with time-varying delay," *IEEE Transactions on Cybernetics*, vol. 53, no. 5, pp. 3376–3387, 2023.

[3] R. B. Zadeh, A. Zaslavsky, S. W. Loke, and S. MahmoudZadeh, "A multiagent mission coordination system for continuous situational awareness of bushfires," *IEEE Transactions on Automation Science and Engineering*, vol. 20, no. 2, pp. 1275–1291, 2023.

[4] L. Cao, Z. Cheng, Y. Liu, and H. Li, "Event-based adaptive NN fixed-time cooperative formation for multiagent systems," *IEEE Transactions on Neural Networks and Learning Systems*, vol. 29, no. 12, pp. 3936–3946, 2021.

[5] C. Chen, W. Zou, and Z. Xiang, "Leader-following connectivity-preserving consensus of multiple euler-Lagrange systems with disturbances," *IEEE Systems Journal*, pp. 1–10, 2023.

[6] C. Wang, J. Wang, C. Zhang, Y. Du, Z. Liu, and C. L. P. Chen, "Fixed-time event-triggered consensus tracking control for uncertain nonlinear multiagent systems with dead-zone constraint," *International Journal of Robust and Nonlinear Control*, vol. 33, no. 11, pp. 6151–6170, 2023.

[7] Y. Shang, B. Chen, and C. Lin, "Consensus tracking control for distributed nonlinear multiagent systems via adaptive neural backstepping approach," *IEEE Transactions on Systems, Man, and Cybernetics: Systems*, vol. 50, no. 7, pp. 2436–2444, 2020.

[8] L. Zhang, B. Chen, and C. Lin, "Adaptive neural consensus tracking control for a class of 2-order multi-agent systems with nonlinear dynamics," *Neurocomputing*, vol. 404, pp. 84–92, 2020.

[9] H. Wang, W. Yu, W. Ren, and J. Lü, "Distributed adaptive finite-time consensus for second-order multiagent systems with mismatched disturbances under directed networks," *IEEE Transactions on Cybernetics*, vol. 51, no. 3, pp. 1347–1358, 2021.

[10] H. Du, G. Wen, G. Chen, J. Cao, and F. E. Alsaadi, "A distributed finite-time consensus algorithm for higher-order leaderless and leader-following multiagent systems," *IEEE Transactions on Systems, Man, and Cybernetics: Systems*, vol. 47, no. 7, pp. 1625–1634, 2017.

[11] X. Liu, J. Lam, W. Yu, and G. Chen, "Finite-time consensus of multiagent systems with a switching protocol," *IEEE Transactions on Neural Networks and Learning Systems*, vol. 27, no. 4, pp. 853–862, 2016.

[12] G. Li, X. Wang, and S. Li, "Finite-time output consensus of higher-order multiagent systems with mismatched disturbances and unknown state elements," *IEEE Transactions on Systems, Man, and Cybernetics: Systems*, vol. 49, no. 12, pp. 2571–2581, 2019.

[13] A. Polyakov, "Nonlinear feedback design for fixed-time stabilization of linear control systems," *IEEE Transactions on Automatic Control*, vol. 57, no. 8, pp. 2106–2110, 2012.

[14] Z. Zuo, Q. L. Han, B. Ning, X. Ge, and X. M. Zhang, "An overview of recent advances in fixed-time cooperative control of multiagent systems," *IEEE Transactions on Industrial Informatics*, vol. 14, no. 6, pp. 2322–2334, 2018.

[15] J. Liu, Y. Zhang, Y. Yu, H. Liu, and C. Sun, "A zeno-free self-triggered approach to practical fixed-time consensus tracking with input delay," *IEEE Transactions on Systems, Man, and Cybernetics: Systems*, vol. 52, no. 5, pp. 3126–3136, 2022.

[16] J. Ni, Y. Tang, and P. Shi, "A new fixed-time consensus tracking approach for second-order multiagent systems under directed communication topology," *IEEE Transactions on Systems, Man, and Cybernetics: Systems*, vol. 51, no. 4, pp. 2488–2500, 2021.

[17] Y. Liu, F. Zhang, P. Huang, and Y. Lu, "Fixed-time consensus tracking for second-order multiagent systems under disturbance," *IEEE Transactions on Systems, Man, and Cybernetics: Systems*, vol. 51, no. 8, pp. 4883–4894, 2021.

[18] L. Zhang, B. Chen, C. Lin, and Y. Shang, "Fuzzy adaptive fixed-time consensus tracking control of high-order multiagent systems," *IEEE Transactions on Fuzzy Systems*, vol. 30, no. 2, pp. 567–578, 2022.

[19] J. Wang, Q. Gong, K. Huang, Z. Liu, C. L. P. Chen, and J. Liu, "Event-triggered prescribed settling time consensus

compensation control for a class of uncertain nonlinear systems with actuator failures," *IEEE Transactions on Neural Networks and Learning Systems*, pp. 1–11, 2021.

[20] J. Gao, Z. Fu, and S. Zhang, "Adaptive fixed-time attitude tracking control for rigid spacecraft with actuator faults," *IEEE Transactions on Industrial Electronics*, vol. 66, no. 9, pp. 7141–7149, 2019.

[21] H. Wang, P. X. Liu, X. Zhao, and X. Liu, "Adaptive fuzzy finite-time control of nonlinear systems with actuator faults," *IEEE Transactions on Cybernetics*, vol. 50, no. 5, pp. 1786–1797, 2020.

[22] Y. Yin, F. Wang, Z. Liu, and Z. Chen, "Finite-time leader-following consensus of multiagent systems with actuator faults and input saturation," *IEEE Transactions on Systems, Man, and Cybernetics: Systems*, vol. 52, no. 5, pp. 3314–3325, 2022.

[23] G. Song, P. Shi, and C. P. Lim, "Distributed fault-tolerant cooperative output regulation for multiagent networks via fixed-time observer and adaptive control," *IEEE Transactions on Control of Network Systems*, vol. 9, no. 2, pp. 845–855, 2022.

[24] Y. Zhang and F. Wang, "Adaptive neural control of non-strict feedback system with actuator failures and time-varying delays," *Applied Mathematics and Computation*, vol. 362, Article ID 124512, 2019.

[25] Y. Yu, J. Guo, and Z. Xiang, "Distributed fuzzy consensus control of uncertain nonlinear multiagent systems with actuator and sensor failures," *IEEE Systems Journal*, vol. 16, no. 3, pp. 3480–3487, 2022.

[26] Y. Zhang, H. Li, J. Sun, and W. He, "Cooperative adaptive event-triggered control for multiagent systems with actuator failures," *IEEE Transactions on Systems, Man, and Cybernetics: Systems*, vol. 49, no. 9, pp. 1759–1768, 2019.

[27] Z. Chen, J. Wang, T. Zou, K. Ma, and Q. Wang, "Adaptive 2-bits-triggered neural control for uncertain nonlinear multiagent systems with full state constraints," *Neural Networks*, vol. 153, pp. 37–48, 2022.

[28] C. Chen, W. Zou, and Z. Xiang, "Event-triggered consensus of multiple uncertain euler–Lagrange systems with limited communication range," *IEEE Transactions on Systems, Man, and Cybernetics: Systems*, vol. 53, no. 9, pp. 5945–5954, 2023.

[29] C. Wang, J. Wang, Y. Du, C. Zhang, Z. Liu, and C. Philip Chen, "Fixed-time event-triggered fuzzy adaptive control for uncertain nonlinear systems with full-state constraints," *Information Sciences*, vol. 633, pp. 158–169, 2023.

[30] J. Wang, C. Wang, C. L. P. Chen, Z. Liu, and C. Zhang, "Fast finite-time event-triggered consensus control for uncertain nonlinear multiagent systems with full-state constraints," *IEEE Transactions on Circuits and Systems I: Regular Papers*, vol. 70, no. 3, pp. 1361–1370, 2023.

[31] C. Zhang, Z. Chen, J. Wang, Z. Liu, and C. L. P. Chen, "Fuzzy adaptive two-bit-triggered control for a class of uncertain nonlinear systems with actuator failures and dead-zone constraint," *IEEE Transactions on Cybernetics*, vol. 51, no. 1, pp. 210–221, 2021.

[32] Y. Wang, Y. Song, and F. L. Lewis, "Robust adaptive fault-tolerant control of multiagent systems with uncertain non-identical dynamics and undetectable actuation failures," *IEEE Transactions on Industrial Electronics*, vol. 62, no. 6, pp. 1–3988, 2015.

[33] Y. X. Li, "Command filter adaptive asymptotic tracking of uncertain nonlinear systems with time-varying parameters and disturbances," *IEEE Transactions on Automatic Control*, vol. 67, no. 6, pp. 2973–2980, 2022.

[34] Y. X. Li, X. Hu, W. Che, and Z. Hou, "Event-based adaptive fuzzy asymptotic tracking control of uncertain nonlinear systems," *IEEE Transactions on Fuzzy Systems*, vol. 29, no. 10, pp. 3003–3013, 2021.

[35] L. Xing, C. Wen, Z. Liu, H. Su, and J. Cai, "Event-triggered adaptive control for a class of uncertain nonlinear systems," *IEEE Transactions on Automatic Control*, vol. 62, no. 4, pp. 2071–2076, 2017.

[36] X. Hu, Y. X. Li, and Z. Hou, "Event-triggered fuzzy adaptive fixed-time tracking control for nonlinear systems," *IEEE Transactions on Cybernetics*, vol. 52, no. 7, pp. 7206–7217, 2022.

[37] X. Jin, "Adaptive fixed-time control for MIMO nonlinear systems with asymmetric output constraints using universal barrier functions," *IEEE Transactions on Automatic Control*, vol. 64, no. 7, pp. 3046–3053, 2019.

[38] H. Wang, K. Xu, and J. Qiu, "Event-triggered adaptive fuzzy fixed-time tracking control for a class of nonstrict-feedback nonlinear systems," *IEEE Transactions on Circuits and Systems I: Regular Papers*, vol. 68, no. 7, pp. 3058–3068, 2021.

[39] Y. Wang, Y. Song, and W. Ren, "Distributed adaptive finite-time approach for formation–containment control of networked nonlinear systems under directed topology," *IEEE Transactions on Neural Networks and Learning Systems*, vol. 29, no. 7, pp. 3164–3175, 2018.